Heat Treatment and Characterization of Nb_3Sn Strands for the Model Coil of the 40-T Hybrid Magnet

P. He, Z. M. Chen, W. G. Chen, and Y. F. Tan

***Abstract*—A model coil for the 40-T hybrid magnet is being built at the Chinese High Magnetic Field Laboratory, Chinese Academy of Sciences. Nb_3Sn/restack-rod-process (RRP) strands adopted for the model coil were heat-treated according to the heat treatment (HT) schedule recommended by the manufacturer, which is Oxford Superconducting Technology. The microstructure of the reacted strand was analyzed. Measurements of the critical current, the residual resistivity ratio and the hysteresis losses were also carried out. The results of critical-characteristic measurements confirmed that the performance of the heat-treated wire was good. All characteristics indicated that the HT of the Nb_3Sn/RRP strands was successfully completed.**

***Index Terms*—Heat treatment (HT), hysteresis losses, magnet, Nb_3Sn.**

I. Introduction

THE 40-T hybrid magnet has been designed at the Chinese High Magnetic Field Laboratory (CHMFL), Chinese Academy of Sciences, Hefei, China. According to the design of the 40-T hybrid magnet, a superconducting outsert composed of superconducting coils connected in series will be responsible for generating a magnetic field of 11 T, whereas the resistive insert will generate a high field of 29 T. The superconducting outsert is divided into four subcoils. The inner three subcoils will be layer-wound using different grades of Nb_3Sn cable-in-conduit conductors (CICC), and the outer one will be wound by Nb_3Sn CICC pancakes. All the superconducting coils will be cooled by 4.5-K force-flowed supercritical helium [1]. In order to ensure the feasibility of the design, a model coil has been designed and is being manufactured to develop the techniques of cabling, jacketing, winding, and heat treatment (HT) for the 40-T hybrid magnet. The main design parameters and specifications are listed in Table I. The conductor of the model coil will be the same Nb_3Sn CICC conductors as the outsert of the 40-T hybrid magnet [2].

The critical current density was required to be high in order to provide the required performance of the magnet and to keep the magnet as compact as possible. Among several types of Nb_3Sn strands, the one most promising for us is the internal-tin Nb_3Sn strands, for they can carry relatively high current densities of more than $\sim$2100 A/mm^2 at 12 T and 4.2 K. In our magnet, we adopted the high-current restack-rod-process (RRP) strand from Oxford Superconducting Technology (OST) for its great performance of non-Cu critical-current-density values. Nb_3Sn is formed by an HT from a strand containing only metallic components such as Nb, Sn, Cu, Ti, and Ta [3]. An HT to form the superconducting phase by solid-state diffusion is required. Not only the temperature but also the duration of the HT determines the grain structure in the filaments of the strands. Hence, physical properties such as the critical current and the residual resistivity ratio (RRR) value can be optimized if a good HT is carried out. Consequently, the HT of the Nb_3Sn strand is a significant issue for us to design and fabricate the magnet using the superconducting wires.

TABLE I
PARAMETERS OF THE MODEL COIL

Strand type	Nb_3Sn
Cable pattern	(2Sc+1Cu)×4×4×4
Jacket material	Stainless steel 316LN
Jacket wall thickness	1.6 mm
Conductor outer dimensions	24.2 mm×10.3 mm
Void fraction	30%
Winding type	Layer
Inner diameter of the winding	120.4 mm
Outer diameter of the winding	266 mm
Height of the winding	529.2 mm

Five groups of Nb_3Sn strand samples were heat-treated by using the vacuum HT system. Then, the Nb_3Sn-sample characteristics, such as the critical current, the hysteresis losses, and the RRR, were measured. The obtained results showed that this type of Nb_3Sn strand basically met the required properties at high magnetic field. This paper includes the details of the strand HT and the results of the performance measurements.

II. Experiments

A. Strand Descriptions

Nb_3Sn superconducting wires made by the RRP were used for this study. This RRP technique consists of stacking Cu-clad Nb rods around a Sn core. Each filament bundle (subelement) has its own Sn core and is surrounded by a Nb diffusion barrier that acts to prevent the diffusion of Sn into the copper matrix during the reaction [4]. It is essential for obtaining a high current-carrying capacity to ensure a good diffusion of Sn into Nb to produce Nb_3Sn at near stoichiometric composition

Manuscript received August 25, 2010; revised September 6, 2010 and September 29, 2010; accepted October 1, 2010. Date of publication November 12, 2010; date of current version December 3, 2010. This paper was recommended by Associate Editor P. Lee.

The authors are with the Superconducting Magnets Group, Chinese High Magnetic Field Laboratory, Chinese Academy of Sciences, Hefei 230031, China (e-mail: hepengcas@163.com).

Color versions of one or more of the figures in this paper are available online at http://ieeexplore.ieee.org.

Digital Object Identifier 10.1109/TASC.2010.2085045

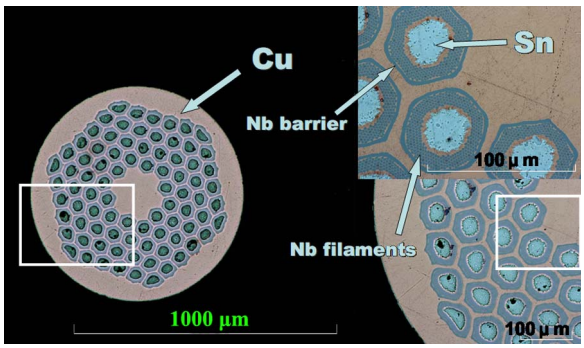

Fig. 1. Cross-sectional overview of the unreacted Nb_3Sn/RRP superconducting strand 11451-1.

Fig. 2. Preparation of the superconducting strand samples before the HT. (Top) Straight samples for RRR tests. The coils at the bottom were used in the I_c measurements and hysteresis losses.

throughout the entire A15 volume [5]. The cross-sectional overview of this wire is shown in the Fig. 1. The wire has a Cu matrix as the stabilizer, and 84 hexagonal subelements are embedded in the Cu matrix. The diameter of the strand is 0.81 mm, and the thickness of the chrome plating is 1.17 μm.

B. Sample Preparation and Heat Treatment Procedure

Five samples for I_c measurements were wound onto Ti6Al4V barrel sample holders before the HT. The I_c barrel, which consists of two copper rings at two ends, is 32 mm in diameter and is 30 mm in height. The thermal expansion coefficients of Ti and Nb_3Sn are similar; therefore, the residual thermal stress in the Nb_3Sn strand is reduced. The critical current was measured by the standard four-point method. During the measurements, the sample temperature was kept constant at 4.2 K, and then, a dc was applied to the strand and increased from zero. These measurements were carried out under different background fields, i.e., 12, 13, and 14 T. The critical current was defined by the criterion of 10 μV/m.

Five sets of samples were prepared and heat-treated for this study; they were fixed to different sample holders and numbered as 11473-3, 11422-3, 11470-1, 11451-1, and 11447-2 for the test of the hysteresis losses, the I_c measurement, and the RRR value, respectively, as shown in Fig. 2. The samples to be used for I_c measurements were wound on grooved cylindrical barrels made of a Ti6Al4V alloy. All the sample holders were installed onto the sample bar of the HT furnace system before the HT. The furnace chamber is cylindrical, its diameter is 200 mm, and its length is 600 mm.

We were supposed to carry out the HT of the strands in Ar gas because the outsert coil would be also heat-treated in the future in the same condition; therefore, it was meaningful for us to get the consultative information about the this procedure. However, as is known to all, the temperature uniformity is the one of the most essential conditions for the HT. Unfortunately, we were unable to achieve the required temperature uniformity of ± 5 °C in the Ar gas condition, while the required temperature uniformity in the vacuum was easy to be satisfied. Therefore, we heat-treated the Nb_3Sn strands in the vacuum for this test to ensure the temperature uniformity in the furnace chamber. We know that the effect of the HT in Ar is much better than that in the vacuum because there are much fewer impurities that are harmful to the superconducting strands during the HT.

The HT of Nb_3Sn strands in the vacuum can also provide a relatively clean circumstance to reduce the amount of impurities released from the coil or the insulation, such as O_2 and carbon-hydrogen gas, which will pollute the Nb_3Sn during the high-temperature diffusion reaction to affect the performance of the Nb_3Sn after the HT. For the HT of the sample strands, there are fewer impurities than the model coil and the 40-T outsert coil, and there are no insulations or cable conduits; therefore, vacuum circumstances can satisfy the HT requirement, while in the HT of the model coil and the 40-T outsert coil, maintaining Ar gas in the HT furnace is necessary because the more-strict condition of environmental cleanness should be met. We required that the vacuum level during the HT should be better than 1×10^{-3} Pa so that the HT process could be carried out in vacuum conditions. We also tested that the temperature uniformity in the working area of this furnace was better than ± 5 °C.

A successful HT requires that the samples and the fittings of the furnace should be clean; particularly, they should not be contaminated with oil. Because carbon-hydrogen gas can be decomposed from the oil during the high temperature of the HT, meanwhile, the gas will react with the Nb_3Sn in the high-temperature environment leading the degradation of the critical performance of Nb_3Sn. To achieve these conditions, we first cleaned the chamber of the furnace. The furnace was pumped to 1×10^{-2} Pa, held for 15 min, and flushed with argon gas. This process was repeated twice.

We planned to heat-treat the samples according to the schedule recommended by the manufacturer, which is OST. The entire process of the HT was automatically recorded by a computer data acquisition system. Three thermocouples were installed near the samples to record the sample temperatures accurately. However, the furnace temperature was controlled by another three thermocouples located on the wall of the furnace chamber. Therefore, a problem occurred at the first period of the entire procedure, as can be seen from Fig. 3, when the temperature of the samples lagged behind the temperature-controlling thermocouples in the low-temperature stage. We accordingly increased the dwelling time of the first dwelling stage by 2 h to offset the difference between the sample temperature and the furnace-wall temperature. After the first temperature stage, the difference between them was negligible, so we continued the HT according to the original schedule.

The first temperature dwelling stage was 210 °C. The recommended dwelling time is 48 h, but we increased it to 50 h as described above. The increase in dwelling time follows the OST recommendation that the dwelling time should be increased if

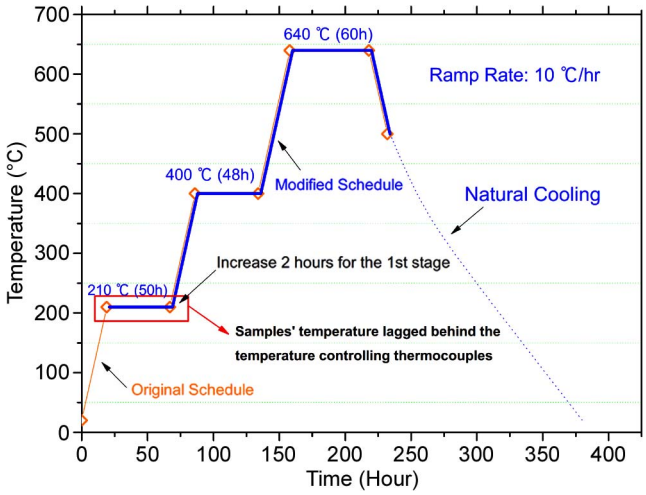

Fig. 3. Modified HT schedule of Nb_3Sn/RRP strands.

there is a significant error in the temperature uniformity. After the first temperature stage was finished, the temperature ramped up at 10 °C/h to the second temperature stage at 400 °C, where the dwelling time was 48 h. After the second temperature stage was finished, we continued to ramp up the temperature to the next temperature stage of 640 °C with the same rate, and dwelled for 60 h. Finally, the temperature was ramped down to 500 °C at 10 °C/h. When the temperature reached 500 °C, the temperature was allowed to decrease to room temperature at the time constant of the furnace plus the samples. Fig. 3 depicts the HT schedule that we followed.

III. Test Results and Discussion

A. Microstructure Analysis of the Strand

Nb_3Sn/RRP is a type of internal-tin Nb_3Sn strand. The internal-tin process has advantages compared with other methods of manufacturing Nb_3Sn strands, such as the bronze process. Due to using very ductile elements such as Nb, Sn, Ta, and Cu, the internal-tin process is less complicated in terms of mechanical deformation. In addition, intermediate stress-relief annealing is not required, whereas it is a necessary procedure for the bronze technique strand.

In general, the formation of the internal-tin Nb_3Sn requires a series of thermal processes, i.e., low-temperature diffusion at ∼210 °C, which is responsible for forming bronze by Sn and Cu, followed by the intermediate temperature diffusion at ∼400 °C where more Cu–Sn phases are formed, and lastly, the formation of the intermetallic Nb_3Sn grain occurs through the high-temperature diffusion at ∼640 °C.

Five groups of strand samples were analyzed by the electronic microscopy of the strand cross sections. Each test sample was prepared as follows. First, strands samples were embedded in epoxy modules, and then, the modules were polished for many times using an abrasive paper with various grits. After polishing, the samples were located on an optical microscope to get the detailed images of the strand cross section.

Fig. 4 shows the cross-sectional microstructural image and analysis of strand sample 11447-2 after the HT. The Nb_3Sn-

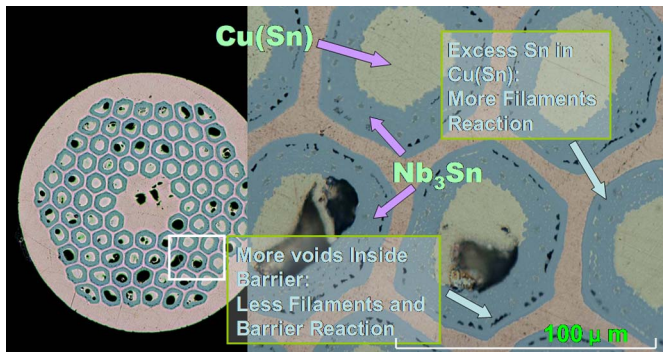

Fig. 4. Cross-sectional microstructural image of heat-treated strand sample 11447-2.

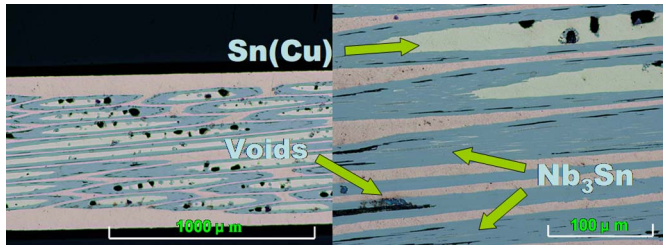

Fig. 5. Longitudinal-section microstructural image of heat-treated strand sample 11447-2.

strand HT is one of the key technical operations for achieving high critical current density because the Nb_3Sn superconducting layer is created by high-temperature solid-diffusion reaction. It can be clearly seen from the images that the parts with different colors of the strands represent different strand components. The red part represents the Cu matrix, whereas the light-blue parts are subelements with the Nb rods and the Sn core. The large voids in the subelements reflect the phenomenon that the Sn source diffuses to the Nb rods during the HT. We speculate that the reaction of Nb and Sn near the regions with the large voids is more completely finished.

As shown in the images, the excess Sn located in the barrier leads to more filaments' reaction to form more Nb_3Sn grains, which are propitious to improve the critical current density, while subelements with relatively more voids show less Sn diffusion into the Nb filaments and the Nb barrier, which causes less formation of the Nb_3Sn grain boundaries leading to low current-carrying capacities compared with the subelement mentioned above. The image of the longitude section of strand 11447-2 is also given in Fig. 5.

It should also be noted that there are many dark-gray rods among the Nb rods in the subelements. They are the ternary additions to Nb_3Sn, such as Ti or Ta, which are employed widely in practical conductors. Both Ti- and Ta-containing conductors have been developed to improve J_c in the high-field region. Moreover, it is also reported that addition of Ta to the filament prevents sausaging and is useful for suppression of ac losses [6].

On one hand, we can generally conclude that the quality of the HT to the Nb_3Sn strand is good from the microscopic photographs we got because there are no broken subelements or obvious Sn diffusion out of the Nb barrier and little deformation

TABLE II
MAIN RESULTS OF CHARACTERISTICS MEASUREMENTS OF THE Nb_3Sn SAMPLES. I_c AT 12 T AND 4.2 K; RRR AT 0 T AND 285 K/20 K

Strand No.	RRR	J_c (A/mm^2)	n
11447-2	164	2108	38.6
11451-1	59	2026	37.9
11473-3	75	2123	42.4
11470-1	60	2026	39.7
11422-3	47	2150	46.1

of subelements is observed. This conclusion is reflected in the results of the critical-current test described in Section III-B. On the other hand, there are still many aspects to improve, such as the temperature homogeneity of the operating region and maintaining a high vacuum in the furnace chamber during the HT. Finally, we conclude that the results are good enough to allow us to carry out the HT of Nb_3Sn conductors and coils on the model coil in the near future.

B. Critical Current and RRR

There were five strand samples for the critical-current measurement. The critical currents of all samples ranged from 522 A to 554 A @12 T and, 4.2 K ($J_c \sim 2026$ to 2150 A/mm^2), and the n-values ranged from 38 to 49, which meets the procurement requirements ($J_c \sim 2100$ A/mm^2; n-value > 20). The results of the RRR measurements and the calculated values of J_c and the n-value are shown in the Table II.

As for the RRR measurements, the current of 1 A was applied to the samples in order to test their resistance at temperatures of 285 K and 20 K. According to Table II, it is noticeable that, except for the sample 11447-2, whose RRR value of which is relatively normal, the RRR values of the other four samples are somewhat lower. We speculate that it is in connection with the location in the furnace chamber during the HT. Since the control thermocouple measures the temperature of the chamber wall, the control thermocouple reads a significantly higher temperature than the monitoring thermocouple, and these strands were located too close to the wall of the furnace chamber or to the heater of the furnace leading to a phenomenon that Sn first completely reacts with Nb and then diffuses out of the Nb barrier and into the Cu matrix to contaminated the Cu matrix Cu, consequently, the RRR value was relatively low.

C. Hysteresis Losses

The hysteresis losses of five samples were measured using a Quantum Design MPMS XL-7 hysteresis loss measurement system. We calculated the hysteresis losses during the quasi-static −6.8 T–0–6.8-T field cycle, and the results meet the requirement that the hysteresis losses should be less than 1600 kJ/m^3. The measurement temperature is 4.22 K. Before the measurements, we made the strands to the shape of spiral, whose diameter of which is 5 mm, and the number of turns was 6 ∼ –7. We measured hysteresis loops at different field ramp rates from 0.001 T/s to 0.003 T/s.

It can be seen in Fig. 6 that flux jumping occurs at the low- field region of the curves. For this type of Nb_3Sn strand,

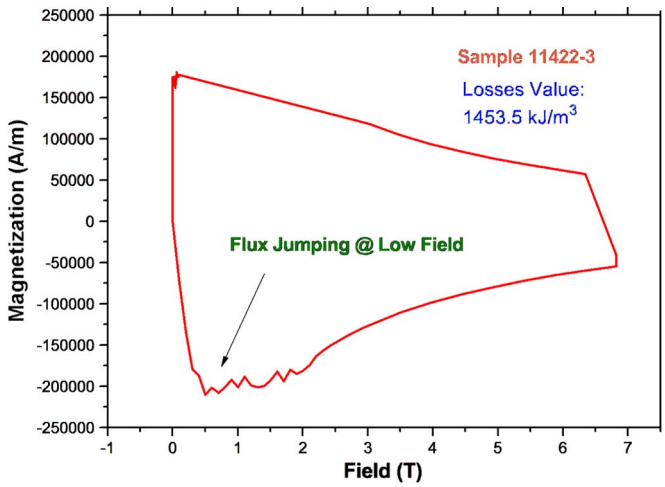

Fig. 6. Magnetization curves as a function of the applied field for the Nb_3Sn strand sample 11422-3.

the filament diameter is effectively the sub-element diameter, which is 70 μm, and the combination of this large effective filament diameters and high current densities makes the flux jumps at low fields, which are inevitable. Although the good cooling condition by He gas maintains the sample temperature at 4.22 K, the flux jumps always exist always in the lower-fields region because, at low fields, the energy contained in the critical state can exceed the heat capacity, a condition that is not adiabatically stable and even a small disturbance can trigger massive collapse of the critical state and can cause the quench. And this phenomenon not only relates to the cooling condition but also to the quench mechanism, especially (particularly) in the low field. While at the high field, the magnetic energy in the critical state is lower than the heat capacity, quenching only occurs when the current approaches the critical current [7]. It can be concluded that improving the stability in the low field is as important as that in the high field.

IV. CONCLUSION

The model coil for the 40-T hybrid magnet hais being been being built at the High Magnetic Field Laboratory, Chinese Academy of Sciences (CHMFLCHMFL). It is has been being wound with CICCs using Nb_3Sn/RRP with high J_c value. Five strand samples were have been heat-treated according to the schedule recommended by the manufacturer. By the analysis of microstructure for the reacted strands, we have concluded that there was almost no Sn leakage or sub-element breakage that could reduce the critical performance of the strands. After the HT, strand samples were have been measured for the critical current, as well as"" for the hysteresis losses.

The critical current densities were have been also calculated and ranged from 2026 to 2150 A/mm^2 @12 T, 4.2 K, and the hysteresis losses ranged from 1446 to 1546 kJ/m^3; therefore, they have met the requirements of the strand specifications. With respect to the RRR value, four samples got somewhat lower, which have been speculated as the Sn diffusion out of the Nb barrier to contaminate the Cu matrix caused by local overheat in the furnace chamber during the HT, and we have

planned to repeat the measurement in the near future. In general, the performance of Nb_3Sn/RRP strands heat-treated by the recommended schedule have met the fundamental requirements for us to utilize them to fabricate the CICCs that will be wound into the model coil of the 40-T hybrid magnet. Future work will explore the performance of the CICC conductor in the model coil fabricated of the same strands by the wind-and-react technique.

REFERENCES

[1] Y. F. Tan, F. T. Wang, Z. M. Chen, Y. N. Pan, and G. L. Kuang, "The design of cable-in-conduit conductors for the superconducting outsert coils of a 40 T hybrid magnet," *Supercond. Sci. Technol.*, vol. 22, no. 2, p. 025 010, Jan. 2009.

[2] Y. F. Tan, W. Chen, Y. Pan, F. Wang, Z. Chen, J. Zhu, and G. Kuang, "A conceptual design of model coil for the 40-T hybrid magnet superconducting outsert," *IEEE Trans. Appl. Supercond.*, vol. 19, no. 6, pp. 3790–3793, Dec. 2009.

[3] H. Muller and Th. Schneider, "Heat treatment of Nb_3Sn conductors," *Cryogenics*, vol. 48, no. 7/8, pp. 323–330, Jul./Aug. 2008.

[4] N. Cheggour, "Influence of Ti and Ta doping on the irreversible strain limit of ternary Nb_3Sn superconducting wires made by the restacked-rod process," *Supercond. Sci. Technol.*, vol. 23, no. 5, p. 052 002, May 2010.

[5] P. J. Lee and D. C. Larbalestier, "Microstructural factors important for the development of high critical current density Nb_3Sn strand," *Supercond. Sci. Technol.*, vol. 48, no. 7/8, pp. 283–292, Jul. 2008.

[6] A. David, *Handbook of Superconducting Materials*. Bristol, U.K.: IOP, 2003.

[7] A. K. Ghosh, "Dynamic stability threshold in high-performance internal-tin Nb_3Sn superconductors for high field magnets," *Supercond. Sci. Technol.*, vol. 18, no. 1, pp. L5–L8, Jan. 2005.

P. He was born in 1983. He is a doctoral student in the Chinese High Magnetic Field Laboratory, Chinese Academy of Sciences (CHMFL), Hefei, China.

He is engaged in research on the characteristics of Nb_3Sn superconducting magnets and strand, especially CICC superconducting outsert of the hybrid magnet which is being built at CHMFL. Additionally, he is involved with the heat treatment of the Nb_3Sn CICC conductors which are critical technical parts in the construction of the hybrid magnet.

Z. M. Chen was born in 1943.

He is a Professor in the Chinese High Magnetic Field Laboratory, Chinese Academy of Sciences, Hefei, China. He is engaged in research on techniques and applications of superconducting magnets. He is also engaged in the technical diagnosis of tokamak devices.

W. G. Chen was born in 1976. He graduated from Hefei Technology University, China, in 1995. He also received the Master's degree in mechanical engineering. He received the Ph.D. degree from the Institute of Plasma Physics, Chinese Academy of Sciences, China, in 2002.

He is a Professor in the Chinese High Magnetic Field Laboratory, Chinese Academy of Sciences, Hefei, China. His main interests are fusion science and technology. His current research field is superconducting magnet technology and structure design. He visited the Japan National Institute of Fusion Science and has participated in several international scientific conferences.

Y. F. Tan received the Ph.D. degree.

He is an Associate Professor in the Chinese High Magnetic Field Laboratory, Chinese Academy of Sciences, Hefei, China. He is engaged in research on the characteristics and measurements of superconducting magnets.